Incorporation of Low-dimensional Materials into the Two-dimensional Interlamellar Nanospace of a Pillared Interlayered Solid

Kunio Ohtsuka* and Yoshimasa Hayashi

Electronics Technology Research Center, Mitsubishi Materials Corporation, 2270 Yokoze, Yokoze-machi, Chichibu, 368-8503 Japan

Received May 31, 2000. Revised Manuscript Received October 17, 2000

We studied the synthesis of nanostructured oxide/hydroxide within the two-dimensional nanospace of a pillared interlayered solid (alumina-pillared clay). A nickel(II) hydroxide unit layer was introduced into the pore of the pillared clay by adding a base to a nickel(II) nitrate solution containing the pillared clay calcined over 300 °C. The formation of the low-dimensional nickel(II) hydroxide was evaluated by X-ray diffraction analysis, elemental analysis, surface area measurements, temperature-programmed reduction measurements, and X-ray photoelectron spectroscopy measurements. In situ growth of nanostructured NiO in the pores was performed by the heat treatment of the intracrystalline nickel(II) hydroxide. The Ni 2p binding energy of the intracrystalline nickel(II) hydroxide was the same as that of bulk nickel(II) hydroxide. However, the intracrystalline NiO had a Ni 2p binding energy ca. 2−3 eV higher than that of bulk NiO. These phenomena were rationalized in terms of the structure of the pores of the pillared clay and the structures of nickel(II) hydroxide and NiO. The intracrystalline nickel(II) hydroxide was less reducible than bulk nickel(II) hydroxide; Ni metal was afforded outside the pores upon reduction in hydrogen at 500 °C.

Introduction

Pillared interlayered solids are a new class of microporous solid having two-dimensional nanopores. They are prepared by introducing precursors for metal oxide clusters into the interlayers of layered solids followed by calcination. Because these zeolite-like pillared derivatives may have pore sizes larger than those of zeolites, they have received widespread interest in the field of catalysis and separation.[1−6] Furthermore, the voids of pillared solids may offer a cosseted environment to encapsulate readily degraded substances and volatile materials that are not easy to handle in the air. The voids also can be considered as micro reaction chambers that function as templates.[7]

The approach that introduces a low-dimensional nanophase into the void will serve both as a route to the synthesis of novel hybrid materials and as a route to the modification of pillared interlayered solids that leads to the control of their lateral pore size and chemical properties.

The materials encapsulated in the two-dimensional nanopores of pillared interlayered solids will have nanostructured properties. Nanostructured materials frequently exhibit unusual electrical properties, magnetic properties, and chemical reactivity, but they are inherently unstable, tending to undergo Ostwald ripening in the absence of supports or stabilizing agents.[8] Thus, pillared interlayered solids containing intracrystalline nanostructured materials within the pores may give a better understanding of low-dimensional materials, and will open possibilities to produce novel electronic, optoelectronic, magnetic, and chemical functional devices and elements.

Furthermore, introduction of a nanophase into the pore will enhance the versatility of the pillared solids in catalysis and separation. Modification of pillared interlayered solids [namely, control of lateral pore opening and control of chemical properties (i.e., acidity, affinity, etc.)] is required to give appropriate properties to the solids for use in catalysis and separation.[5,6] Two ways have been adopted to control the lateral pore opening: (1) control of the pillar density through reduced-charge host materials or controlled ion exchange and (2) deposition of a secondary phase into the pores. The latter approach is of interest because it may change the chemical properties together with pore opening, and besides, it may cause high thermal stability. Coke deposition on pillared clays was investigated by Maes and Vansant,[9,10] but their methods resulted in irregular deposition without a controlled pore modification.

* To whom correspondence should be addressed. Present address: 6-42-16 Higashi-ooizumi, Nerima-ku, Tokyo, 178-0063 Japan.

(1) Pinnavaia, T. J. *Science* **1983**, *220*, 365.
(2) Vaughan, D. E. W. *ACS Symp. Ser.* **1988**, *368*, 308.
(3) Burch, R., Ed. *Catal. Today* **1988**, *2*, 1−185.
(4) Mitchell, I. V., Ed. *Pillared Layered Structure: Current Trends and Applications*; Elsevier: London, 1990.
(5) Ohtsuka, K. *Chem. Mater.* **1997**, *9*, 2039.
(6) Cool, P.; Vansant, E. F. *Mol. Sieves* **1998**, *1*, 265.
(7) Cassagneau, T.; Hix, G. B.; Jones, D. J.; Maireles-Torres, P.; Rhomari, M.; Rozière, J. *J. Mater. Chem.* **1994**, *4*, 189.
(8) Hayashi, T.; Ueda, R.; Tasaki, A. *Ultra-fine Particles*; Noyes Publications: Westwood, NJ, 1997.
(9) Maes, N.; Vansant, E. F. *J. Porous Mater.* **1996**, *3*, 257.
(10) Maes, N.; Vansant, E. F. *J. Porous Mater.* **1997**, *4*, 5.

10.1021/cm0004329 CCC: $20.00
Published on Web 02/02/2001

In this study, we propose the preparative procedures for the synthesis of nanostructured oxide/hydroxide within the pores of a pillared interlayered solid (alumina-pillared clay). We prepared an alumina-pillared clay containing intracrystalline nickel(II) hydroxide by the titration method. We discuss the mechanism of the preferential growing of the hydroxide within the pores along with the possibility of achieving a controlled pore modification. Moreover, we have illustrated transformations of the intracrystalline nickel(II) hydroxide to NiO, metal, and semiconductor metal sulfide (MeS). At the same time, we have described some low-dimensional characteristics of the intracrystalline nickel(II) hydroxide/oxide within the pores.

Experimental Section

Synthesis of a Pillared Interlayered Solid. We chose an alumina-pillared mica as the starting pillared interlayered solid having two-dimensional pores, because it has high thermal stabilities and high surface areas. The alumina-pillared clay was prepared as follows. Into 750 mL of a 0.2 M aluminum(III) chloride solution, 3750 mL of a 0.072 M sodium hydroxide solution was added at a rate of 5 mL/h using a microtubing pump to achieve an OH/Al mole ratio of 1.8. This partially hydrolyzed Al solution was aged at 95 °C for 48 h, and then cooled to room temperature. This solution contains the Al_{13} polynuclear cations that become pillars between the silicate layers upon intercalation. To this solution, 15 g of sodium fluoride tetrasilicic mica was added to yield an Al/mica ratio of 1 mol of Al/100 g of clay, and it was mixed vigorously for 24 h at room temperature. Next, the resulting product was collected and washed thoroughly by centrifugation, and then dried at 105 °C for 24 h. Subsequently, the intercalate was calcined at different temperatures (150, 200, 300, 400, and 500 °C) for 4 h. These heat-treated products are called alumina-pillared clays here, although the Al_{13} polynuclear cations do not dehydrate and dehydroxylate completely to oxide pillars below 300 °C. Distilled−deionized water was used for all the experimental work.

Sodium fluoride tetrasilicic mica ($NaMg_{2.5}Si_4O_{10}F_2$) was used as the host clay for the alumina-pillared clay because of its high thermal stabilities and high crystallinity. A commercially available 10 wt % sol of sodium fluoride tetrasilicic mica from Topy Industries was diluted with water, and impurities [α-quartz and magnesium fluoride richterite ($Na_2Mg_6F_2(Si_4O_{11})_2$] were removed by conventional centrifugal sedimentation techniques. The purified sol was then condensed with an evaporator and finally dried at 105 °C. Sodium fluoride tetrasilicic mica has a 2:1 layered structure: the two tetrahedral sublayers contain Si^{4+}; the central octahedral sublayer contains Mg^{2+}. Sodium ions exist between the silicate layers to compensate for the negative layer charge arising from a deficiency of Mg^{2+} in the octahedral sublayer. The theoretical cation-exchange capacity is 254 mequiv/100 g of clay. Further details concerning the characteristics of the silicate are described elsewhere.[11]

Synthesis of an Alumina-pillared Clay with Intracrystalline Nickel(II) Hydroxide. *Titration*. Titration curves were used to assess the possibility of introducing nickel(II) hydroxide into the two-dimensional nanospace of the pillared clay. The titration was performed in the following way: Three grams of the alumina-pillared clay calcined at 500 °C was added to 200 mL of a 0.1 M nickel(II) nitrate solution and stirred for 2 d. Next, this suspension was titrated potentiometrically under stirring by dropwise addition of a 0.1 M sodium hydroxide solution (400 mL) using a microtubing pump at a rate of 1 mL/h. The change in pH was monitored continuously using a combination glass electrode.

(11) Ohtsuka, K.; Hayashi, Y.; Suda, M. *Chem. Mater.* **1993**, *5*, 1823.

Synthesis of an Alumina-pillared Clay with Intracrystalline Nickel(II) Hydroxide. Effect of calcining temperatures of the pillared clay on the synthesis was investigated. Three grams of the alumina-pillared clay calcined at desired temperatures (150, 200, 300, 400, and 500 °C) was added to 200 mL of a 0.1 M nickel(II) nitrate solution, and then stirred for 2 d. Next, the suspensions were titrated under stirring by a dropwise addition of a 0.1 M sodium hydroxide solution using a microtubing pump at a rate of 1 mL/h to obtain OH/Ni ratios of 0.1, 0.2, 0.3, 0.4, 0.5, 0.6, and 0.7, respectively, and kept stirring for 1 week. Finally, the resulting products were collected and washed repeatedly by centrifugation, and then dried at 105 °C for 24 h.

Removal of Isolated Nickel(II) Hydroxide. Isolated nickel(II) hydroxide that was produced during the titration procedures was dissolved preferentially by hydrochloric acid washing.The amount of the isolated nickel(II) hydroxide was small; most of nickel(II) hydroxide was deposited in the pores of the pillared clay during the titration procedures. This will be explained in detail later.

The conditions of the dissolution, which were determined by preliminary experiments, were as follows: A 0.3-g sample of the product obtained by the titration treatment was mixed with 50 mL of a 0.01 M hydrochloric acid solution, stirred for 30 min at 30 °C, and collected by centrifugal techniques. The residue was washed thoroughly with water and dried at 105 °C for 24 h.

Hydrogen Reduction. A 0.5-g sample of the product obtained by the titration treatment followed by acid washing was heated in the air at 500 °C for 2 h and then cooled to the room temperature. The calcined product was then subjected to a reduction treatment at 500 °C in a hydrogen stream of 100 mL/min (the temperature had been increased from the room temperature to 500 °C with a heating rate of 10 °C/min), and cooled to the room temperature. After replacing hydrogen gas with carbon dioxide gas, the product was removed from the furnace.

Characterization. Transmission electron microscope (TEM) analyses were performed with a Philips model CM20 at accelerating voltage of 200 kV. X-ray diffraction (XRD) analyses were done with a Rigaku model RINT-2000. Surface areas were measured with a Carlo Elba model Sorptomatic Series 1800 using N_2 gas adsorption. X-ray photoelectron spectroscopy (XPS) measurements were performed with a Physical Electronics model 5600LS, and binding energies for this work were referenced to C 1s (284.8 eV). Temperature-programmed reduction (TPR) measurements were done as follows: A 100-mg sample of the products resulting from the titration treatment was charged into a quartz tube reactor and heated with a heating rate of 10 °C/min in reducing gas (5% hydrogen in argon) flow. A trap, cooled with methanol/dry ice, was placed after the reactor, and water vapor in the outlet gas formed during reduction was removed. The outlet gas was continuously analyzed with a thermal conductivity detector attached to a Hitachi model 263-50 gas chromatograph. The area enclosed by the TPR peaks corresponds to the amount of the reducible species in the sample.

Results and Discussion

Titration. Figure 1 shows pH titration curves obtained by titrating nickel(II) nitrate solutions in the presence and in the absence of the alumina-pillared clay with a sodium hydroxide solution. In the nickel(II) nitrate solution without the pillared clay, upon addition of the base, the pH of the solution rose rapidly and reached the solubility product, which allowed the immediate precipitation of nickel(II) hydroxide. In contrast, in the nickel(II) nitrate solution containing the pillared clay calcined at 500 °C, the titration curve in the range of from OH/Ni = 0 (no NaOH added) to point A (OH/Ni = ca. 0.7) lied below the curve of the nickel(II) nitrate solution without the pillared clay. This

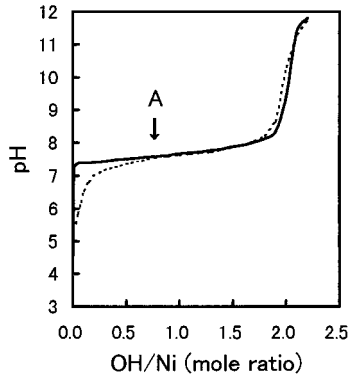

Figure 1. pH titration curves obtained by titrating 0.1 M nickel(II) nitrate solutions in the presence (dashed line) and in the absence (solid line) of an alumina-pillared clay calcined at 500 °C with a 0.1 M sodium hydroxide solution.

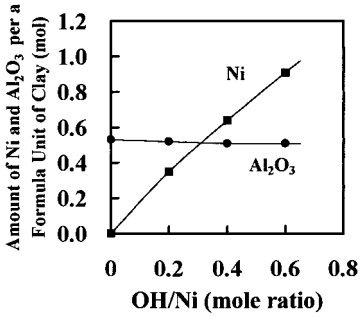

Figure 2. Elemental analysis of Ni and Al_2O_3 in products obtained by a titration treatment using an alumina-pillared clay calcined at 500 °C. The values shown at OH/Ni = 0 were derived from the pillared clay before the titration treatment.

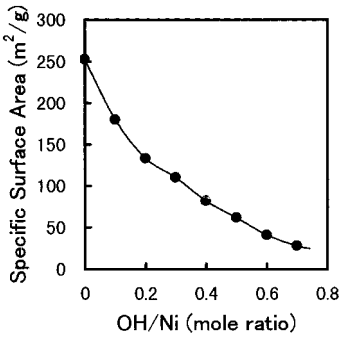

Figure 3. BET surface areas for products obtained by a titration treatment using an alumina-pillared clay calcined at 500 °C. The value shown at OH/Ni = 0 was derived from the pillared clay before the titration treatment.

implies that in this range of titration, nickel(II) hydroxide precipitates not in the solution, but in the pores of the alumina-pillared clay.

Alumina-pillared Clay with Intracrystalline Nickel(II) Hydroxide. Figure 2 shows the elemental analyses of the products obtained by the titration treatment at various stages using the alumina-pillared clay calcined at 500 °C. The amount of Ni precipitated increased almost stoichiometrically with the addition of alkali, that is, with an increase in the OH/Ni ratio, whereas the amount of alumina did not change before and after titration. As shown in Figure 3, Brunauer−Emmett−Teller (adsorption isotherm) (BET) surface areas decreased from 253 m^2/g (OH/Ni = 0) to 28 m^2/g (OH/Ni = 0.7) with an increase in the OH/Ni ratio, which

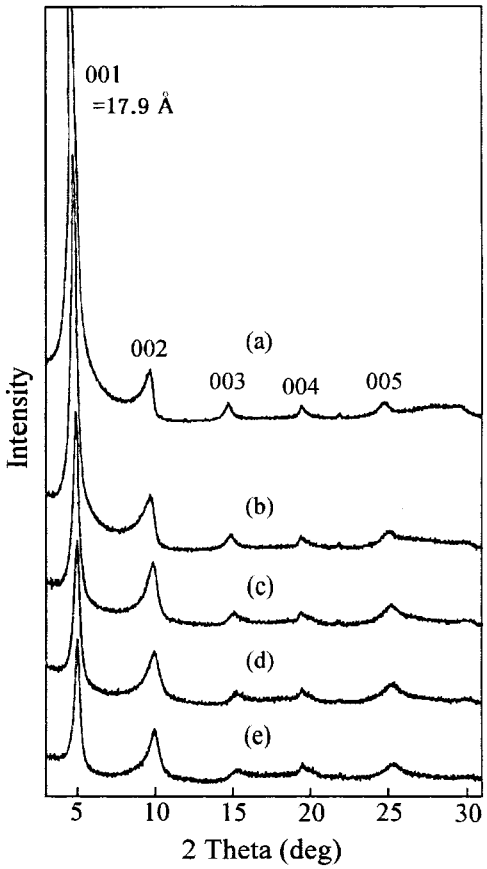

Figure 4. XRD profiles for products obtained by a titration treatment using an alumina-pillared clay calcined at 500 °C: OH/Ni = (a) 0, (b) 0.2, (c) 0.4, (d) 0.6, and (e) 0.7. The profile shown at OH/Ni = 0 was derived from the pillared clay before the titration treatment.

suggests a progressive deposition of nickel(II) hydroxide in the pores of the pillared clay.

No free nickel(II) hydroxide was detected in the XRD profiles for the reaction products (Figure 4). As indicated in Figure 2, the amount of Ni precipitated at OH/Ni = 0.6 was 0.91 mol, corresponding to 16.4 wt % of $Ni(OH)_2$, which is large enough to be observed in our XRD studies if it exists outside the pores. Hence, nickel(II) hydroxide was considered to be precipitated preferentially in the pores of the pillared clay. To be precise, 6% of the precipitated $Ni(OH)_2$ was formed outside the pores. This was revealed by TPR measurements and will be explained later.

Furthermore, the XRD spectra illustrated that the basal spacings of the resulting products were almost constant (=17.9 Å), whereas the 001 intensity decreased with an increase in the OH/Ni ratio. We believe, from previous XRD studies for a nickel(II) hydroxide-2:1 clay intercalation compound that has a chlorite-like structure (Figure 5c),[12,13] that these facts suggest that a nickel(II) hydroxide layer developed in the two-dimensional space of the pillared clay by the titration treatment, although alumina-pillared clays have alumina clusters between the silicate layers. The previous XRD analyses showed that, as a nickel(II) hydroxide

(12) Ohtsuka, K.; Suda, M.; Tsunoda, M.; Ono, M. *Chem. Mater.* **1990**, *2*, 511.
(13) Ohtsuka, K.; Suda, M.; Ono, M.: Takahashi, M.; Sato, M.; Ishio, S. *Bull. Chem. Soc. Jpn.* **1987**, *60*, 871.

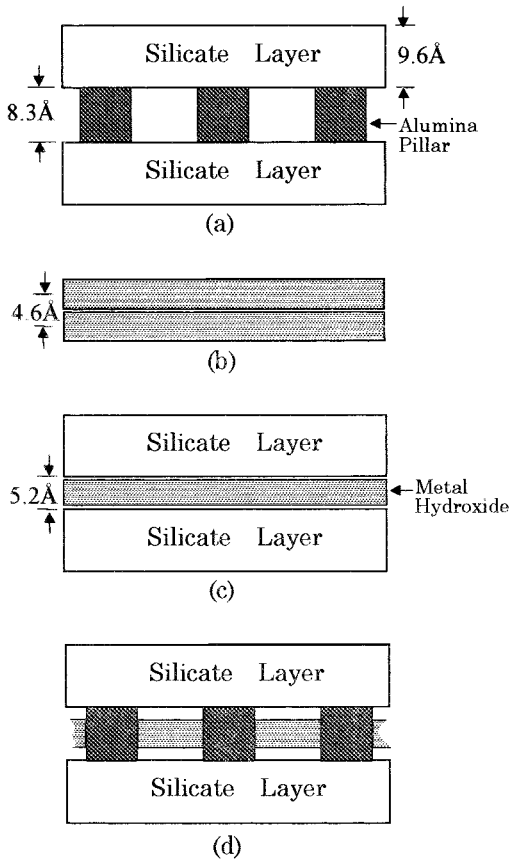

Figure 5. Schematic representation of the structures of (a) the alumina-pillared clay calcined at 500 °C used in this study, (b) nickel(II) hydroxide with the CdI_2 layer structure, (c) a chlorite-like metal hydroxide-2:1 layer silicate intercalation compound, and (d) an alumina-pillared clay with intracrystalline nickel(II) hydroxide.

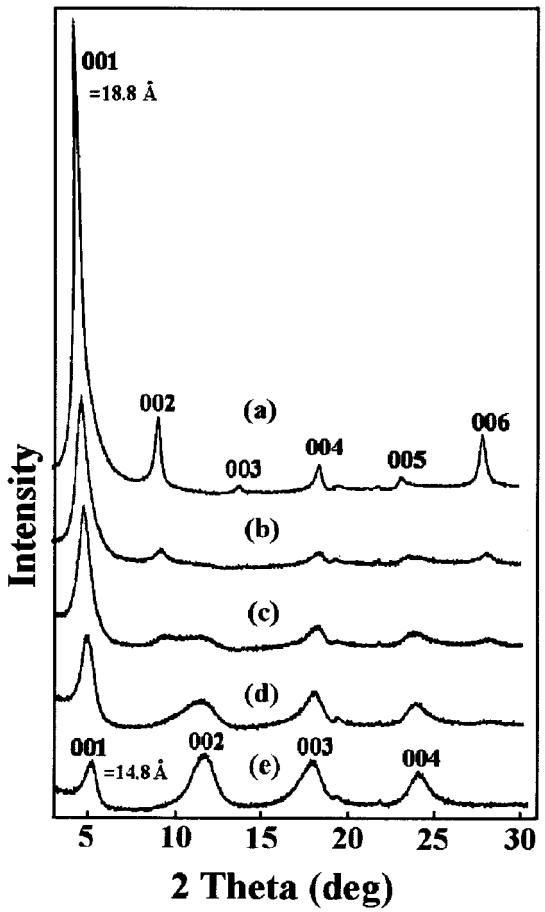

Figure 6. XRD profiles for products obtained by a titration treatment using an alumina-pillared clay calcined at 150 °C: OH/Ni = (a) 0, (b) 0.2, (c) 0.4, (d) 0.6, and (e) 0.7. The profile shown at OH/Ni = 0 was derived from the pillared clay before the titration treatment.

interlayer develops between the silicate layers of 2:1 clay, X-ray intensity of the 001 reflection for the intercalate decreases, but the 002−004 intensities increase. Nickel(II) hydroxide crystallize with the CdI_2 layer structure, consisting of a superposition of a brucite-like nickel(II) hydroxide unit layer (Figure 5b). The products prepared by the titration treatment have the nickel(II) hydroxide unit layer within the pores. Figure 5d illustrates a schematic structure of the resulting products, that is, an alumina-pillared clay with intracrystalline nickel(II) hydroxide. The titration treatment for the pillared clays calcined at more than 300 °C resulted in the same products.

In contrast, the alumina-pillared clay calcined at 300 °C or below yielded different products after the titration treatment. Elemental analyses of the products obtained by the titration treatment using the alumina-pillared clay calcined at 150 °C demonstrated that the amount of Ni increased almost stoichiometrically with the addition of alkali, but the amount of alumina did not change. BET surface areas for the products decreased with the progress of titration from 240 m^2/g (OH/Ni = 0) to 35 m^2/g (OH/Ni = 0.7).[14] The trends for these variations in elemental analyses and BET surface areas resemble those observed for the pillared clay calcined at 500 °C: nickel(II) hydroxide was considered to be deposited preferentially in the pore of the pillared clay calcined at 150 °C.

Figure 6 shows XRD profiles for the products obtained using the pillared clay calcined at 150 °C with the progress of titration. No free nickel(II) hydroxide was detected in the profiles. With an increase in the OH/Ni ratio, the 001 intensity decreased, and the higher order 002−004 intensities increased. These changes in X-ray intensities coincided with those with the interlayering of nickel(II) hydroxide for a nickel(II) hydroxide-2:1 clay intercalation compound having a chlorite-like structure, as stated earlier. Moreover, interlayer spacing [= 001 basal spacing − layer thickness (9.6 Å)] varied drastically from 9.2 Å (OH/Ni = 0) to 5.2 Å (OH/Ni = 0.7). Chlorite-like structures have approximately 001 basal spacings of 14−15 Å (= interlayer spacings of 4−5 Å). It is confirmed, therefore, that as titration proceeds, the alumina pillars calcined at 150 °C decompose by alkali, forming a Ni(II)−Al(III) hydroxide layer (brucite−gibbsite-like layer) between the silicate layers. Both nickel(II) and aluminum(III) hydroxides have the CdI_2 layer structure and have a solid solution between them. The structure of the final resulting product at OH/Ni =

(14) The BET surface area of the calcined at 150 °C is almost the same as that of the calcined at 500 °C, although the basal spacing decreased from 18.8 Å (at 150 °C) to 17.9 Å (at 500 °C), corresponding to a decrease in the longitudinal pore size (gallery height) from 9.2 to 8.3 Å. This is because the lateral pore size of the calcined at 500 °C is larger than that of the calcined at 150 °C: dehydration and dehydroxylation of the Al_{13} ion goes to completion at more than 300 °C.

0.7 is composed of silicate layers and a brucite−gibbsite-like interlayer; that is, a metal hydroxide-layer silicate intercalation compound having a chlorite-like structure (Figure 5c). The titration treatment for the pillared clays calcined between 150 and 300 °C resulted in the same products.

It is thus revealed that a nickel(II) hydroxide layer grows preferentially in the pores of the alumina-pillared clay calcined at more than 300 °C by the titration method without destroying the pillars.

Mechanism of Preferential Precipitation of Nickel(II) Hydroxide in the Pores of an Alumina-Pillared Clay. Pillared clays exhibit cation and anion exchange properties depending on the pH of the exchanging solution.[15−19] Dyer and Gallardo first investigated the ion-exchange properties of alumina- and zirconia-pillared clays; they learned that the capacity predominantly arises from contributions by the pillars.[15] They proposed that the exchange reactions occur owing to the amphoteric character of surface hydroxyl groups of the rehydrated pillars in solution, in a way similar to the hydrated surface of oxides. The hydroxyl groups of the pillars function as a proton donor (cation exchanger) at high pH, and as a proton acceptor (anion exchanger) at low pH. In fact, Kukkadapu and Kevan[19] showed that Cu^{2+} ions are sorbed onto the pillars of an alumina-pillared clay calcined at 350 °C.

Hachiya et al.[20] and de Bokx et al.[21] showed that hydrated Ni^{2+} ion is adsorbed coordinately on the surface hydroxyl group of alumina at high pH as follows:

$$-\mathrm{AlOH} \rightarrow -\mathrm{AlO}^- + \mathrm{H}^+ \quad (1)$$

(dissociation of surface hydroxyl group)

$$-\mathrm{AlO}^- + [\mathrm{Ni(OH_2)_6}]^{2+} \rightarrow -\mathrm{AlONi(OH_2)_5}^+ + \mathrm{H_2O} \quad (2)$$

(coordination adsorption of Ni^{2+} ion)

$$-\mathrm{AlONi(OH_2)_5}^+ \rightarrow -\mathrm{AlONi(OH)(OH_2)_4} + \mathrm{H}^+ \quad (3)$$

(surface hydrolysis of the adsorbed metal ion)

We think the preferential development of a nickel(II) hydroxide layer in the pores of the pillared clay takes place as follows: First, upon mixing an alumina-pillared clay with a nickel(II) nitrate solution, Ni^{2+} ions are adsorbed on the surface of alumina pillars, and protons are released by surface hydrolysis in a way similar to alumina. Subsequently, a nickel(II) hydroxide layer develops preferentially within the pore, as in the metal hydroxide interlayering process between the silicate layers of 2:1 clays,[12,22] in the following way. The released protons in the pore exchange with Ni^{2+} ions in solution, which accounts for the fact that the pH value of the nickel(II) nitrate solution containing an alumina-pillared clay is lower than that of the nickel(II) nitrate solution without the pillared clay (Figure 1). The coordinated water of the Ni^{2+} ions introduced into the pore is dissociated by polarization caused by the combined effect of the positive charge of the Ni^{2+} ion and the negative layer charge of the silicate layer,[23] and releases protons. Upon addition of a base to the suspension, the protons in solution are neutralized, further hydrolysis of Ni^{2+} ions in the pore proceeds, and polynuclear hydroxonickel(II) complexes develop around the pillars by the olation between the hydrolyzed nickel ions and the hydrated Ni^{2+} ions coordinately adsorbed on the pillar. A nickel(II) hydroxide layer grows around the pillars by a repetition of this process, and eventually the pore is completely occupied with nickel(II) hydroxide. The progressive growth of nickel(II) hydroxide around the pillars may lead to a controlled pore-narrowing. In this study, we used mica, but it is apparent that this method can be applied to alumina-pillared clays based on other host materials, for example, montmorillonite, saponite, and so on.

Upon heating, the pillaring precursor (Al_{13} ion) is converted to alumina, water, and charge-balancing protons,[24] and then the protons migrate into the octahedral framework.[25−27] Thus, the protons locked within the clay sheets are not exchangeable under normal ion-exchange conditions. However, the treatment of the calcined pillared clay with a base such as ammonia restores the cation-exchange capacity; the base is able to abstract the trapped protons and transfer them, as NH^{4+} ions, to the silicate surface.[27−29] In our experimental conditions, that is the titration treatment in the range of from OH/Ni = 0 to point A in Figure 1, such restoring reactions are unlikely to occur because sodium hydroxide added to the suspensions is readily consumed to form nickel(II) hydroxide, and consequently pH values are retained in neutral regions (pH < 7.5).[30]

In short, the two-dimensional pore of the pillared clay functions as a template for the low-dimensional syn-

(15) Dyer, A.; Gallardo, T. In *Recent Developments in Ion Exchange*; Williams, P. A., Hudson, M. J., Eds.; Elsevier: Amsterdam, 1990; Vol. 199, p 75.
(16) Clearfield, A.; Aly, H. M.; Cahill, R. A.; Serrette, G. P. D.; Shea, W. L.; Tsai, T. Y. In *Zeolites and Microporous Crystals* (*Proceedings of ZMPC 93*); Hattori, T., Yashima, T., Eds.; Kodansha/Elsevier: Tokyo, 1994; p 433.
(17) Nava-Galve, G.; Pacheco, G.; Fetter, G.; Bosch, P.; Bulbulian, S. *J. Radioanal. Nucl. Chem.* **1996**, *207*, 263.
(18) Ahenach, J.; Cool, P.; Vansant, E. F. *Microporous Mater.* **1998**, *26*, 185.
(19) Kukkadapu, R. K.; Kevan, L. *J. Phys. Chem.* **1988,** *92*, 6073.
(20) Hachiya, K.; Sasaki, M.; Saruta, Y.; Mikami, N.; Yasunaga, T. *J. Phys. Chem.* **1984**, *88*, 23.
(21) de Bokx, P. K.; Wassenberg, W. B. A.; Geus, J. W. *J. Catal.* **1987**, *104*, 86.
(22) Yamanaka, S.; Brindley, G. W. *Clays Clay Miner.* **1978**, *26*, 21.
(23) The mica used in this study has a higher negative layer charge than do smectites and, consequently, 22% (0.22 mol of Na) of the charge-balancing Na ions remained in the clay after exchange with the Al_{13} ions. Hence, even after proton diffusion by heating the clay with the Al_{13} ions, the silicate layer has a negative layer charge corresponding to 22% of that of the original clay. Montmorillonite derives its cation exchange capacity (CEC) mainly from substitution of Mg^{2+} for Al^{3+} in the octahedral sites. But usually a contribution to the CEC from substitution of Al^{3+} for Si^{4+} in the tetrahedral sites cannot be bypassed. Hence, even after proton diffusion by heating the clay with the Al_{13} ions, localized negative layer charge may exist on the silicate layer, although the layer charge is neutralized in total by protons.
(24) Vaughan, D. E. W.; Lussier, R. J. In *Proceedings of the 5th International Conference on Zeolites*; Rees, L. V. C., Ed.; Heyden: London, 1980; p 94.
(25) Russell, J. D.; Fraser, A. R. *Clays Clay Miner.* **1971**, *19*, 55.
(26) Yariv, S.; Heller-Kallai, L. *Clays Clay Miner.* **1973**, *21*, 199.
(27) Tennakoon, D. T.; Jones, W.; Thomas, J. M. *J. Chem. Soc., Faraday Trans. 1* **1986**, *82*, 3081.
(28) Vaughan, D. E. W.; Lussier, R. J.; Magee, J. S., Jr. U.S. Patent 4 271 043, 1981.
(29) Molinard, A.; Cool, P.; Vansant, E. F. *Microporous Mater.* **1994**, *3*, 149.
(30) Even if the restoring is the case here during our titration procedures, it makes no difference in the mechanism of the growth of nickel(II) hydroxide within the pore. The Ni^{2+} ions introduced into the pores by the restored cation-exchange property of the clay layer behave like the Ni^{2+} ions introduced by the ion exchange with protons.

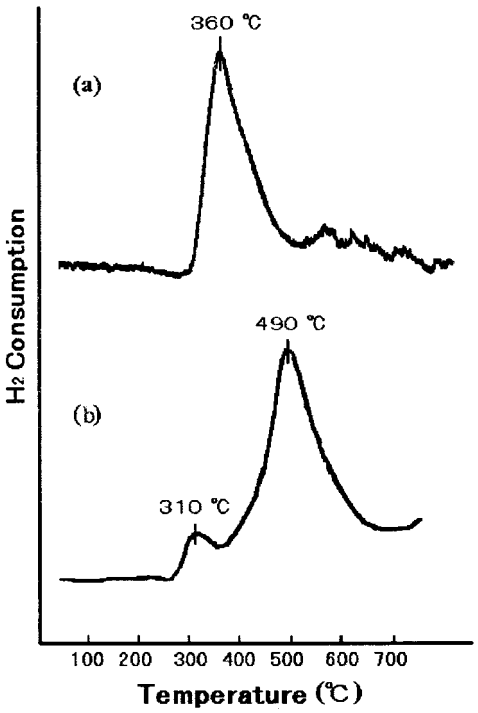

Figure 7. TPR profiles for (a) bulk nickel(II) hydroxide obtained by a titration treatment in the absence of an alumina-pillared clay, and (b) a product obtained by a titration treatment with OH/Ni = 0.5 using an alumina-pillared clay calcined at 500 °C.

thesis; nickel(II) hydroxide has a layered structure to be accommodated in the two-dimensional, spatially restricted region. The ion-exchange properties of the pillar and the acidic character of the pillared clay are responsible for the preferential formation of the hydroxide layer within the pores.

It is assumed that not only Ni(II) hydroxide but also Mg(II), Ca(II), Mn(II), Fe(II), Co(II), Zn(II), Cd(II), and Al(III) hydroxides are introduced into the pore of the pillared clay by the same titration treatment, because these hydroxides can crystallize with the CdI_2 layer structure and are intercalated between the silicate layers of 2:1 clays.[12] Furthermore, in situ formation of nanostructured semiconductor metal sulfides (MeS) will be afforded by H_2S treatment of these transition metal (Mn(II), Fe(II), Co(II), Ni(II), Zn(II), and Cd(II) hydroxides at low temperatures.

Reduction Behavior of Intracrystalline Nickel(II) Hydroxide in the Pores of an Alumina-pillared Clay. TPR measurements revealed that the nickel(II) hydroxide in the pore of the pillared clay is less reducible than bulk nickel(II) hydroxide. As shown in Figure 7, the reduction peak of bulk nickel(II) hydroxide was observed at about 360 °C, whereas two reduction peaks at about 310 and 490 °C were found for the products obtained by the titration treatment. The 490 °C peak is due to the reduction of intracrystalline nickel(II) hydroxide in the void of the pillared clay. The 310 °C peak is due to the reduction of isolated nickel(II) hydroxide. The reduction peak temperature of the isolated nickel(II) hydroxide is lower than that of bulk nickel(II) hydroxide, implying that the isolated nickel(II) hydroxide has high dispersion, low crystallinity, and small grain diameter.

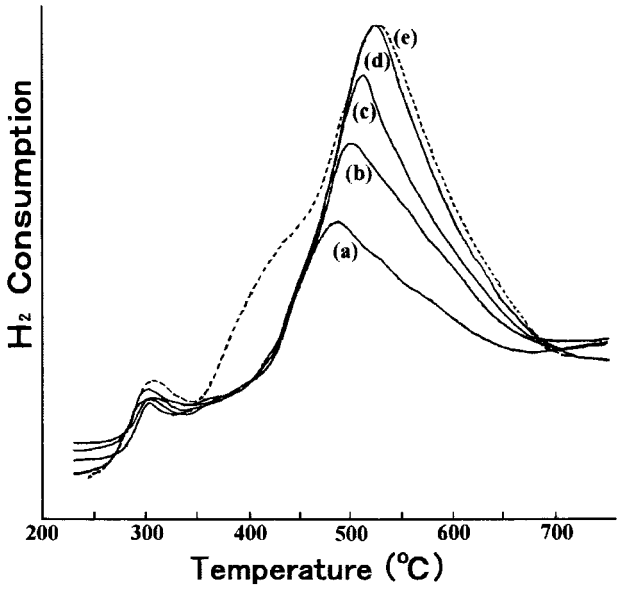

Figure 8. TPR profiles for products obtained by a titration treatment using an alumina-pillared clay calcined at 500 °C: OH/Ni = (a) 0.3, (b) 0.5, (c) 0.6, (d) 0.7, and (e) 1.0.

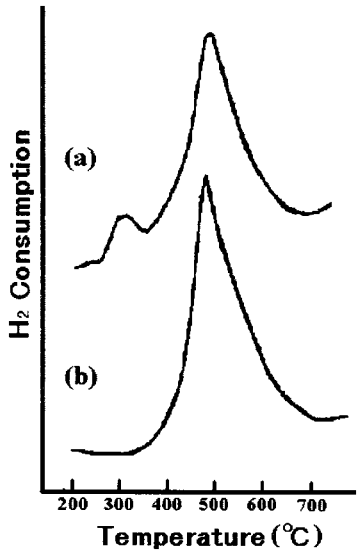

Figure 9. TPR profiles of products obtained by a titration treatment with OH/Ni = 0.5 using an alumina-pillared clay calcined at 500 °C: (a) before and (b) after acid washing.

Figure 8 shows TPR profiles for the products obtained by the titration treatment, as titration proceeds. With the development of nickel(II) hydroxide in the void of the pillared clay (namely, with an increase in the OH/Ni ratio), the reduction peak temperatures were shifted to higher temperatures. As mentioned earlier, nickel(II) hydroxide grows preferentially in the void of the alumina-pillared clay in the range from OH/Ni = 0 to point A (OH/Ni = ca. 0.7). Figure 8e indicates that the product prepared with OH/Ni = 1.0 gave a shoulder on the left of the main reduction peak, which is attributed to excess nickel(II) hydroxide that cannot be accommodated in the void of the pillared clay.

Hydrochloric acid washing was performed to eliminate the isolated nickel(II) hydroxide with a reduction peak at 310 °C. Figure 9 demonstrates that the free nickel(II) hydroxide was dissolved preferentially by the treatment. As proven by chemical analyses (Table 1),

Table 1. Elemental Analysis of a Resulting Product[a] before and after Acid Washing

	composition[b] (mol)			
	Si	Mg	Al	Ni
before HCl washing	4	2.44	1.02	0.77
after HCl washing[c]	4	2.40	1.00	0.72

[a] Obtained by a titration treatment with OH/Ni = 0.5 using an alumina-pillared clay calcined at 500 °C. The clay used was sodium fluoride tetrasilicic mica, $NaMg_{2.5}Si_4O_{10}F_2$. [b] Normalized per 4 mol of Si: a formula unit of the clay contains 4 mol of Si. [c] Treated by a 0.01 M HCl solution to dissolve separated nickel(II) hydroxide.

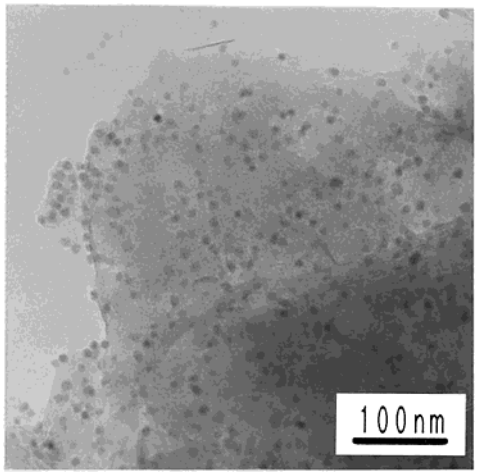

Figure 10. A TEM photograph of a reduced alumina-pillared clay with intracrystalline nickel(II) hydroxide in hydrogen at 500 °C for 1 h. The pillared clay complex was obtained by a titration treatment with OH/Ni = 0.5 using an alumina-pillared clay calcined at 500 °C followed by acid washing.

the acid washing leached out approximately 6% of the nickel(II) hydroxide precipitated by the titration treatment. No perceptible changes in XRD profiles were observed after acid leaching.

According to TEM and XRD analyses, Ni metal particles derived from the reduction of the intracrystalline nickel(II) hydroxide are formed outside the pores. Figure 10 shows that nickel metal formed upon reduction in hydrogen at 500 °C had a particle size of approximately 100 Å in diameter, which is larger than the interlayer spacing (= 8.3 Å). This large particle size resulted from the migration of reduced Ni to the external surfaces of the pillared clay or to the clay defect sites[31,32] created by layer folding, where Ni metal aggregated or sintered to larger particles. XRD measurements showed the existence of nickel metal, whereas the structure of the pillared clay was maintained even after the reduction.

Earlier work on a transition metal carbonyl complex encapsulated in an alumina-pillared clay reports that upon reduction in hydrogen at 400 °C, Ru are formed outside the pores.[31,32] Thus, metal migration at higher temperatures seems to be a general phenomenon; metal formed at high temperatures is not stable in the pores and expelled to the outside of the pores. Mild reduction techniques at low temperatures such as polyol process[33] would result in the formation of metal within the pores.

Upon sufficient exposure of the reduced sample to the air, the nickel metal was oxidized to NiO; the TPR profile of this bulk NiO gave a single reduction peak at 200 °C. On the other hand, the product prepared by calcining an alumina-pillared clay with intracrystalline nickel(II) hydroxide at 500 °C in the air gave a reduction peak at around 500 °C. It became apparent, therefore, that the encapsulated nickel(II) hydroxide converts to NiO in situ in the pore by heat-treatment, and the intracrystalline NiO is less reducible than bulk NiO.

XPS Measurements. Ni 2p ($2p_{3/2}$) binding energy for the alumina-pillared clay with intracrystalline nickel(II) hydroxide (prepared with OH/Ni = 0.5 followed by acid washing) was 855.9 eV, which was almost the same as the value (=855.6 eV) of bulk nickel(II) hydroxide. As stated previously, nickel(II) hydroxide has the CdI_2 layer structure, comprising a superposition of a brucite-like nickel(II) hydroxide unit layer. In the structure of the alumina-pillared clay with intracrystalline nickel(II) hydroxide, the brucite-like unit layer of nickel(II) hydroxide exists in the two-dimensional space of the pillared clay (Figure 5d). Therefore, it is reasonable that there is little difference in the Ni binding energies between bulk nickel(II) hydroxide and the intracrystalline nickel(II) hydroxide grown in the void of the pillared clay.

However, there was a large difference (2−3 eV) in Ni 2p binding energy between the intracrystalline NiO and bulk NiO. Ni 2p binding energy for the alumina-pillared clay with intracrystalline NiO was 856.2 eV; the pillared clay complex was obtained by heating at 500 °C for 1 h the alumina-pillared clay with intracrystalline nickel(II) hydroxide prepared with OH/Ni = 0.5 followed by acid washing. In contrast, Ni 2p binding energy for bulk NiO is 853.5−854.3 eV.[34] This difference in binding energy is rationalized in terms of crystal structures. Nickel(II) oxide crystal has the three-dimensional sodium chloride structure (the rock-salt structure). Because the pillared clay has two-dimensional nanospace with an interlayer spacing of 8.3 Å (Figure 5a), the generated intracrystalline NiO forms a two-dimensional nanophase or low-dimensional small clusters in the void, which accounts for the higher energy shift in the Ni binding energy.

Acknowledgment. We thank the analytical department of the Electronics Technology Research Center for chemical analyses and the Analytical Center of the Central Research Institute for XPS measurements. Thanks are also due to Kazuhiro Akiyama of the Central Research Institute for TEM observations.

CM0004329

(31) Giannelis, E. P.; Rightor, E. G.; Pinnavaia, T. J. *J. Am. Chem. Soc.* **1988**, *110*, 3880.
(32) Pinnavaia, T. J.; Rameswaran, M.; Dimotakis, E. D.; Giannelis, E. P.; Rightor, E. G. *Faraday Discuss. Chem. Soc.* **1989**, *87*, 227.
(33) Fievet, F.; Lagier, J. P.; Blin, B. *Solid State Ionics* **1989**, *32/33*, 198.
(34) Moulder, J. F.; Stickle, W. F.; Sobol, P. E.; Bomben, K. D. *Handbook of X-ray Photoelectron Spectroscopy*; Chastain, J., Ed.; Perkin-Elmer Corporation: Minnesota, 1992.